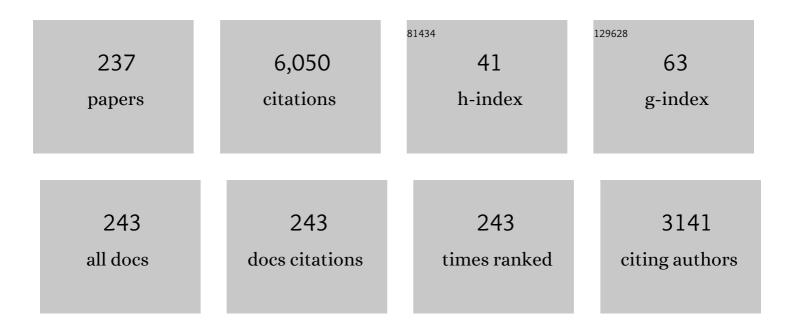
List of Publications by Year in descending order

Source: https://exaly.com/author-pdf/4251741/publications.pdf Version: 2024-02-01



#	Article	IF	CITATIONS
1	Propagation Direction Analyses of Mediumâ€Scale Traveling Ionospheric Disturbances Observed Over North America With GPSâ€TEC Perturbation Maps by Threeâ€Dimensional Spectral Analysis Method. Journal of Geophysical Research: Space Physics, 2022, 127, .	0.8	4
2	Statistical Study of Seasonal and Solar Activity Dependence of Nighttime MSTIDs Occurrence Using the SuperDARN Hokkaido Pair of Radars. Journal of Geophysical Research: Space Physics, 2022, 127, .	0.8	3
3	Detection of Polar Mesospheric Clouds Utilizing Himawariâ€8/AHI Fullâ€Disk Images. Earth and Space Science, 2022, 9, .	1.1	0
4	Relationship between Na layer and CNA variations observed at Syowa, Antarctic. Earth, Planets and Space, 2021, 73, .	0.9	2
5	Role Of the Sun and the Middle atmosphere/thermosphere/ionosphere In Climate (ROSMIC): a retrospective and prospective view. Progress in Earth and Planetary Science, 2021, 8, .	1.1	13
6	Horizontal Movement of Polar Mesospheric Clouds observed from the Himawariâ€8 Geostationary Meteorological Satellite. Journal of Geophysical Research D: Atmospheres, 2021, 126, e2021JD035081.	1.2	2
7	Mesospheric Shortâ€Period Gravity Waves in the Antarctic Peninsula Observed in Allâ€Sky Airglow Images and Their Possible Source Locations. Journal of Geophysical Research D: Atmospheres, 2021, 126, .	1.2	1
8	Relationship between radar cross section and optical magnitude based on radar and optical simultaneous observations of faint meteors. Planetary and Space Science, 2020, 194, 105011.	0.9	4
9	First Direct Observational Evidence for Secondary Gravity Waves Generated by Mountain Waves Over the Andes. Geophysical Research Letters, 2020, 47, e2020GL088845.	1.5	22
10	Wavenumber Spectra of Atmospheric Gravity Waves and Mediumâ€Scale Traveling Ionospheric Disturbances Based on More Than 10‥ear Airglow Images in Japan, Russia, and Canada. Journal of Geophysical Research: Space Physics, 2020, 125, e2019JA026807.	0.8	9
11	Geographical and Seasonal Variability of Mesospheric Bores Observed from the International Space Station. Journal of Geophysical Research: Space Physics, 2019, 124, 3775-3785.	0.8	11
12	Preliminary Dual-Satellite Observations of Atmospheric Gravity Waves in Airglow. Atmosphere, 2019, 10, 650.	1.0	12
13	Observation of Synchronization Between Instabilities of the Sporadic <i>E</i> Layer and Geomagnetic Field Line Connected <i>F</i> Region Mediumâ€Scale Traveling Ionospheric Disturbances. Journal of Geophysical Research: Space Physics, 2019, 124, 4627-4638.	0.8	9
14	Threeâ€Dimensional Fourier Analysis of the Phase Velocity Distributions of Mesospheric and Ionospheric Waves Based on Airglow Images Collected Over 10 Years: Comparison of Magadan, Russia, and Athabasca, Canada. Journal of Geophysical Research: Space Physics, 2019, 124, 8110-8124.	0.8	9
15	Vertical fine structure and time evolution of plasma irregularities in the Es layer observed by a high-resolution Ca+ lidar. Earth, Planets and Space, 2019, 71, .	0.9	10
16	Statistical Analysis of the Phase Velocity Distribution of Mesospheric and Ionospheric Waves Observed in Airglow Images Over a 16â€Year Period: Comparison Between Rikubetsu and Shigaraki, Japan. Journal of Geophysical Research: Space Physics, 2018, 123, 6930-6947.	0.8	15
17	Comparison of gravity wave propagation directions observed by mesospheric airglow imaging at three different latitudes using the M-transform. Annales Geophysicae, 2018, 36, 1597-1605.	0.6	8
18	Initial report on polar mesospheric cloud observations by Himawari-8. Atmospheric Measurement Techniques, 2018, 11, 6163-6168.	1.2	5

#	Article	IF	CITATIONS
19	Comparison of Dust Impact and Solitary Wave Signatures Detected by Multiple Electric Field Antennas Onboard the MMS Spacecraft. Journal of Geophysical Research: Space Physics, 2018, 123, 6119-6129.	0.8	16
20	Effects of Horizontal Wind Structure on a Gravity Wave Event in the Middle Atmosphere Over Syowa (69 [°] S, 40 [°] E), the Antarctic. Geophysical Research Letters, 2018, 45, 5151-5157.	1.5	10
21	Responses of Lower Thermospheric Temperature to the 2013 St. Patrick's Day Geomagnetic Storm. Geophysical Research Letters, 2018, 45, 4656-4664.	1.5	15
22	Simultaneous Observations of Polar Mesosphere Winter Echoes and Cosmic Noise Absorptions in a Common Volume by the PANSY Radar (69.0°S, 39.6°E). Journal of Geophysical Research: Space Physics, 2018, 123, 5019-5032.	0.8	7
23	Historical space weather monitoring of prolonged aurora activities in Japan and in China. Space Weather, 2017, 15, 392-402.	1.3	14
24	Variations of global gravity waves derived from 14Âyears of SABER temperature observations. Journal of Geophysical Research D: Atmospheres, 2017, 122, 6231-6249.	1.2	50
25	Cosmic ray oriented performance studies for the JEM-EUSO first level trigger. Nuclear Instruments and Methods in Physics Research, Section A: Accelerators, Spectrometers, Detectors and Associated Equipment, 2017, 866, 150-163.	0.7	17
26	Characteristics of ripple structures revealed in OH airglow images. Journal of Geophysical Research: Space Physics, 2017, 122, 3748-3759.	0.8	10
27	A scheme for forecasting severe space weather. Journal of Geophysical Research: Space Physics, 2017, 122, 2824-2835.	0.8	28
28	Meteor studies in the framework of the JEM-EUSO program. Planetary and Space Science, 2017, 143, 245-255.	0.9	17
29	Characteristics of mesospheric gravity waves over Antarctica observed by Antarctic Gravity Wave Instrument Network imagers using 3â€Ð spectral analyses. Journal of Geophysical Research D: Atmospheres, 2017, 122, 8969-8981.	1.2	16
30	Simultaneous observation of gravity waves at PMC altitude from AIM/CIPS experiment and PANSY radar over Syowa (69°S, 39°E). Journal of Atmospheric and Solar-Terrestrial Physics, 2017, 164, 324-331.	0.6	6
31	Sixteen year variation of horizontal phase velocity and propagation direction of mesospheric and thermospheric waves in airglow images at Shigaraki, Japan. Journal of Geophysical Research: Space Physics, 2017, 122, 8770-8780.	0.8	21
32	Statistical investigation of Na layer response to geomagnetic activity using resonance scattering measurements by Odin/OSIRIS. Geophysical Research Letters, 2017, 44, 5943-5950.	1.5	3
33	Rayleigh/Raman lidar observations of gravity wave activity from 15 to 70Åkm altitude over Syowa (69ŰS,) Tj ET	Qq]] 0.7	84314 rgBT /(
34	Characteristics of Mesosphere Echoes over Antarctica Obtained Using PANSY and MF Radars. Scientific Online Letters on the Atmosphere, 2017, 13A, 19-23.	0.6	5
35	First mesospheric wind images using the Michelson interferometer for airglow dynamics imaging. Applied Optics, 2016, 55, 10105.	2.1	7
36	Persistent longitudinal variations in 8 years of CIPS/AIM polar mesospheric clouds. Journal of Geophysical Research D: Atmospheres, 2016, 121, 8390-8409.	1.2	9

#	Article	IF	CITATIONS
37	MU radar head echo observations of the 2012 October Draconid outburst. Monthly Notices of the Royal Astronomical Society, 2016, 455, 3273-3280.	1.6	10
38	A mechanism to explain the variations of tropopause and tropopause inversion layer in the Arctic region during a sudden stratospheric warming in 2009. Journal of Geophysical Research D: Atmospheres, 2016, 121, 11,932.	1.2	5
39	Three years of concentric gravity wave variability in the mesopause as observed by IMAP/VISI. Geophysical Research Letters, 2016, 43, 11,528.	1.5	13
40	A scanning Raman lidar for observing the spatio-temporal distribution of water vapor. Journal of Atmospheric and Solar-Terrestrial Physics, 2016, 150-151, 21-30.	0.6	6
41	Special issue "International CAWSES-II Symposium― Earth, Planets and Space, 2016, 68, .	0.9	1
42	Upper Atmosphere Observations by Resonance Scatter Lidars. Journal of the Institute of Electrical Engineers of Japan, 2016, 136, 538-541.	0.0	1
43	Formation of polar ionospheric tongue of ionization during minor geomagnetic disturbed conditions. Journal of Geophysical Research: Space Physics, 2015, 120, 6860-6873.	0.8	19
44	Performances of JEM–EUSO: energy and X max reconstruction. Experimental Astronomy, 2015, 40, 183-214.	1.6	7
45	Calibration aspects of the JEM-EUSO mission. Experimental Astronomy, 2015, 40, 91-116.	1.6	5
46	A sporadic sodium layer event detected with fiveâ€directional lidar and simultaneous wind, electron density, and electric field observation at TromsÃ, Norway. Geophysical Research Letters, 2015, 42, 9190-9196.	1.5	14
47	A thermospheric Na layer event observed up to 140 km over Syowa Station (69.0°S, 39.6°E) in Antarctica. Geophysical Research Letters, 2015, 42, 3647-3653.	1.5	28
48	The infrared camera onboard JEM-EUSO. Experimental Astronomy, 2015, 40, 61-89.	1.6	7
49	Ground-based tests of JEM-EUSO components at the Telescope Array site, "EUSO-TA― Experimental Astronomy, 2015, 40, 301-314.	1.6	16
50	The JEM-EUSO mission: An introduction. Experimental Astronomy, 2015, 40, 3-17.	1.6	38
51	Balloon-borne observations of lower stratospheric water vapor at Syowa Station, Antarctica in 2013. Polar Science, 2015, 9, 345-353.	0.5	8
52	The JEM-EUSO observation in cloudy conditions. Experimental Astronomy, 2015, 40, 135-152.	1.6	10
53	JEM-EUSO: Meteor and nuclearite observations. Experimental Astronomy, 2015, 40, 253-279.	1.6	27
54	Vertical Wind Disturbances during a Strong Wind Event Observed by the PANSY Radar at Syowa Station, Antarctica. Monthly Weather Review, 2015, 143, 1804-1821.	0.5	10

#	Article	IF	CITATIONS
55	The JEM-EUSO instrument. Experimental Astronomy, 2015, 40, 19-44.	1.6	45
56	Height and time characteristics of seasonal and diurnal variations in PMWE based on 1 year observations by the PANSY radar (69.0°S, 39.6°E). Geophysical Research Letters, 2015, 42, 2100-2108.	1.5	16
57	Science of atmospheric phenomena with JEM-EUSO. Experimental Astronomy, 2015, 40, 239-251.	1.6	8
58	The EUSO-Balloon pathfinder. Experimental Astronomy, 2015, 40, 281-299.	1.6	31
59	Performances of JEM-EUSO: angular reconstruction. Experimental Astronomy, 2015, 40, 153-177.	1.6	8
60	Ultra high energy photons and neutrinos with JEM-EUSO. Experimental Astronomy, 2015, 40, 215-233.	1.6	3
61	JEM-EUSO observational technique and exposure. Experimental Astronomy, 2015, 40, 117-134.	1.6	16
62	Variations of nitric oxide in the mesosphere and lower thermosphere over Antarctica associated with a magnetic storm in April 2012. Geophysical Research Letters, 2014, 41, 2568-2574.	1.5	12
63	CME front and severe space weather. Journal of Geophysical Research: Space Physics, 2014, 119, 10,041.	0.8	35
64	A case study of ionospheric storm effects during longâ€lasting southward IMF <i>B_z</i> â€driven geomagnetic storm. Journal of Geophysical Research: Space Physics, 2014, 119, 7716-7731.	0.8	34
65	Atmospheric gravity waves excited by a fireball meteor: Observations and modeling. Journal of Geophysical Research D: Atmospheres, 2014, 119, 8583-8605.	1.2	2
66	Program of the Antarctic Syowa MST/IS radar (PANSY). Journal of Atmospheric and Solar-Terrestrial Physics, 2014, 118, 2-15.	0.6	66
67	New statistical analysis of the horizontal phase velocity distribution of gravity waves observed by airglow imaging. Journal of Geophysical Research D: Atmospheres, 2014, 119, 9707-9718.	1.2	27
68	Groundâ€based observations of nitric oxide in the mesosphere and lower thermosphere over Antarctica in 2012–2013. Journal of Geophysical Research: Space Physics, 2014, 119, 7745-7761.	0.8	8
69	Gravity wave characteristics in the mesopause region revealed from OH airglow imager observations over Northern Colorado. Journal of Geophysical Research: Space Physics, 2014, 119, 630-645.	0.8	20
70	Vertical propagation of a mesoscale gravity wave from the lower to the upper atmosphere. Journal of Atmospheric and Solar-Terrestrial Physics, 2013, 97, 29-36.	0.6	20
71	Inertiaâ€gravity wave in the polar mesopause region inferred from successive images of a meteor train. Journal of Geophysical Research D: Atmospheres, 2013, 118, 3047-3052.	1.2	6
72	The Meteoroid Input Function and predictions of mid-latitude meteor observations by the MU radar. Icarus, 2013, 223, 444-459.	1,1	30

#	Article	IF	CITATIONS
73	An evaluation of the exposure in nadir observation of the JEM-EUSO mission. Astroparticle Physics, 2013, 44, 76-90.	1.9	102
74	Studies of gravity wave propagation in the mesosphere observed by MU radar. Annales Geophysicae, 2013, 31, 845-858.	0.6	3
75	Simultaneous PMC and PMSE observations with a ground-based lidar and SuperDARN HF radar at Syowa Station, Antarctica. Annales Geophysicae, 2013, 31, 1793-1803.	0.6	4
76	MU head echo observations of the 2010 Geminids: radiant, orbit, and meteor flux observing biases. Annales Geophysicae, 2013, 31, 439-449.	0.6	13
77	Decrease in sodium density observed during auroral particle precipitation over TromsÃ, Norway. Geophysical Research Letters, 2013, 40, 4486-4490.	1.5	19
78	TARA: Forward-scattered radar detection of UHECR at the telescope array. EPJ Web of Conferences, 2013, 53, 08012.	0.1	2
79	A meteor head echo analysis algorithm for the lower VHF band. Annales Geophysicae, 2012, 30, 639-659.	0.6	30
80	Adaptive Beamforming Technique for Accurate Vertical Wind Measurements with Multichannel MST Radar. Journal of Atmospheric and Oceanic Technology, 2012, 29, 1769-1775.	0.5	13
81	Mesospheric concentric gravity waves generated by multiple convective storms over the North American Great Plain. Journal of Geophysical Research, 2012, 117, .	3.3	55
82	Comparison of diurnal tide in models and ground-based observations during the 2005 equinox CAWSES tidal campaign. Journal of Atmospheric and Solar-Terrestrial Physics, 2012, 78-79, 19-30.	0.6	20
83	MU radar head echo observations of the 2011 October Draconids. Monthly Notices of the Royal Astronomical Society, 2012, 424, 1799-1806.	1.6	25
84	The 2009-2010 MU radar head echo observation programme for sporadic and shower meteors: radiant densities and diurnal rates. Monthly Notices of the Royal Astronomical Society, 2012, 425, 135-146.	1.6	34
85	Multimodel climate and variability of the stratosphere. Journal of Geophysical Research, 2011, 116, .	3.3	139
86	Long-term observations of the wind field in the Antarctic and Arctic mesosphere and lower-thermosphere at conjugate latitudes. Journal of Geophysical Research, 2011, 116, .	3.3	15
87	Mesopause-region temperature and wind measurements with pseudorandom modulation continuous-wave (PMCW) lidar at 589 nm. Applied Optics, 2011, 50, 2916.	2.1	11
88	First results from the 2009-2010 MU radar head echo observation programme for sporadic and shower meteors: the Orionids 2009. Monthly Notices of the Royal Astronomical Society, 2011, 416, 2550-2559.	1.6	40
89	Air Shower Detection by Bistatic Radar. , 2011, , .		2
90	The increase in OH rotational temperature during an active aurora event. Annales Geophysicae, 2010, 28, 705-710.	0.6	9

#	Article	IF	CITATIONS
91	Mesospheric bore formation from large-scale gravity wave perturbations observed by collocated all-sky OH imager and sodium lidar. Journal of Atmospheric and Solar-Terrestrial Physics, 2010, 72, 7-18.	0.6	29
92	Variability of gravity wave occurrence frequency and propagation direction in the upper mesosphere observed by the OH imager in Northern Colorado. Journal of Atmospheric and Solar-Terrestrial Physics, 2010, 72, 457-462.	0.6	19
93	Variations of OH rotational temperature over Syowa Station in the austral winter of 2008. Earth, Planets and Space, 2010, 62, 655-661.	0.9	3
94	Seasonal and local time variability of ripples from airglow imager observations in US and Japan. Annales Geophysicae, 2010, 28, 1401-1408.	0.6	19
95	MU Radar and Lidar Observations of Clear-Air Turbulence underneath Cirrus. Monthly Weather Review, 2010, 138, 438-452.	0.5	23
96	Simultaneous Observations of Thin Humidity Gradients in the Lower Troposphere with a Raman Lidar and the Very High-Frequency Middle- and Upper-Atmosphere Radar. Journal of Atmospheric and Oceanic Technology, 2010, 27, 950-956.	0.5	8
97	On the consistency of model, groundâ€based, and satellite observations of tidal signatures: Initial results from the CAWSES tidal campaigns. Journal of Geophysical Research, 2010, 115, .	3.3	43
98	Seasonal variation of nocturnal temperature and sodium density in the mesopause region observed by a resonance scatter lidar over Uji, Japan. Journal of Geophysical Research, 2010, 115, .	3.3	9
99	Effects of radar beam width and scatterer anisotropy on multiple-frequency range imaging using VHF atmospheric radar. Radio Science, 2010, 45, n/a-n/a.	0.8	3
100	Simultaneous airglow, lidar, and radar measurements of mesospheric gravity waves over Japan. Journal of Geophysical Research, 2010, 115, .	3.3	25
101	Characteristics of equatorial gravity waves derived from mesospheric airglow imaging observations. Annales Geophysicae, 2009, 27, 1625-1629.	0.6	22
102	Equatorial GPS ionospheric scintillations over Kototabang, Indonesia and their relation to atmospheric waves from below. Earth, Planets and Space, 2009, 61, 397-410.	0.9	10
103	Radar observations of the diurnal tide in the tropical mesosphere-lower thermosphere region: Longitudinal variabilities. Earth, Planets and Space, 2009, 61, 513-524.	0.9	15
104	Wind observation around the tops of the midlatitude cirrus by the MU radar and Raman/Mie lidar. Earth, Planets and Space, 2009, 61, e33-e36.	0.9	5
105	Longitudinal variability in intraseasonal oscillation in the tropical mesosphere and lower thermosphere region. Journal of Geophysical Research, 2009, 114, .	3.3	16
106	Observation of local tidal variability and instability, along with dissipation of diurnal tidal harmonics in the mesopause region over Fort Collins, Colorado (41°N, 105°W). Journal of Geophysical Research, 2009, 114, .	3.3	17
107	Concentric gravity waves in the mesosphere generated by deep convective plumes in the lower atmosphere near Fort Collins, Colorado. Journal of Geophysical Research, 2009, 114, .	3.3	103
108	Critical level interaction of a gravity wave with background winds driven by a largeâ€scale wave perturbation. Journal of Geophysical Research, 2009, 114, .	3.3	9

#	Article	IF	CITATIONS
109	Meteor Orbit Determinations with Multistatic Receivers Using the MU Radar. Earth, Moon and Planets, 2008, 102, 309-314.	0.3	1
110	Atmospheric gravity waves identified by ground-based observations of the intensity and rotational temperature of OH airglow. Polar Science, 2008, 2, 1-8.	0.5	5
111	The 5-8-Day Kelvin and Rossby Waves in the Tropics as Revealed by Ground and Satellite-Based Observations. Journal of the Meteorological Society of Japan, 2008, 86, 43-55.	0.7	5
112	Gravity wave momentum flux in the upper mesosphere derived from OH airglow imaging measurements. Earth, Planets and Space, 2007, 59, 421-428.	0.9	28
113	Development of airglow temperature photometers with cooled-CCD detectors. Earth, Planets and Space, 2007, 59, 585-599.	0.9	13
114	A concentric gravity wave structure in the mesospheric airglow images. Journal of Geophysical Research, 2007, 112, .	3.3	53
115	LowerEregion field-aligned irregularities studied using the Equatorial Atmosphere Radar and meteor radar in Indonesia. Journal of Geophysical Research, 2007, 112, n/a-n/a.	3.3	21
116	An intense gravity wave near the mesopause region observed by a Fabry-Perot interferometer and an airglow imager. Journal of Geophysical Research, 2007, 112, .	3.3	3
117	Semidiurnal tides from the extended Canadian Middle Atmosphere Model (CMAM) and comparisons with TIMED Doppler interferometer (TIDI) and meteor radar observations. Journal of Atmospheric and Solar-Terrestrial Physics, 2007, 69, 2159-2202.	0.6	32
118	Estimation of Humidity Profiles by Combining Co-Located VHF and UHF Wind-Profiling Radar Observation. Journal of the Meteorological Society of Japan, 2007, 85, 301-319.	0.7	6
119	Meteor Orbit Determinations with Multistatic Receivers Using the MU Radar. , 2007, , 309-314.		Ο
120	Simultaneous mesosphere-lower thermosphere and thermosphericFregion observations using middle and upper atmosphere radar. Journal of Geophysical Research, 2006, 111, .	3.3	6
121	Mesospheric gravity waves observed near equatorial and low–middle latitude stations: wave characteristics and reverse ray tracing results. Annales Geophysicae, 2006, 24, 3229-3240.	0.6	32
122	Reverse ray tracing of the mesospheric gravity waves observed at 23°S (Brazil) and 7°S (Indonesia) in airglow imagers. Journal of Atmospheric and Solar-Terrestrial Physics, 2006, 68, 163-181.	0.6	41
123	Observations of the 7-day Kelvin Wave in the Tropical Atmosphere During the CPEA Campaign. Journal of the Meteorological Society of Japan, 2006, 84A, 259-275.	0.7	15
124	A Report on Radar Observations of 5-8-day Waves in the Equatorial MLT Region. Journal of the Meteorological Society of Japan, 2006, 84A, 295-304.	0.7	8
125	A Multi-Instrument Measurement of a Mesospheric Front-Like at the Equator Structure. Journal of the Meteorological Society of Japan, 2006, 84A, 305-316.	0.7	13
126	Lidar Observations of Sporadic Fe and Na Layers in the Mesopause Region over Equator. Journal of the Meteorological Society of Japan, 2006, 84A, 317-325.	0.7	12

#	Article	IF	CITATIONS
127	Simultaneous observation of dual-site airglow imagers and a sodium temperature-wind lidar, and effect of atmospheric stability on the airglow structure. Advances in Space Research, 2005, 35, 1957-1963.	1.2	16
128	Waves in airglow structures experiment 2004: Overview and preliminary results. Advances in Space Research, 2005, 35, 1964-1970.	1.2	5
129	Airglow OH emission height inferred from the OH temperature and meteor trail diffusion coefficient. Advances in Space Research, 2005, 35, 1940-1944.	1.2	10
130	Geomagnetic conjugate observation of nighttime medium-scale and large-scale traveling ionospheric disturbances: FRONT3 campaign. Journal of Geophysical Research, 2005, 110, .	3.3	96
131	Interannual variability of diurnal tide in the tropical mesopause region: A signature of the El Nino-Southern Oscillation (ENSO). Geophysical Research Letters, 2005, 32, .	1.5	52
132	Climatological lower thermosphere winds as seen by ground-based and space-based instruments. Annales Geophysicae, 2004, 22, 1931-1945.	0.6	10
133	Foil chaff ejection systems for rocket-borne measurement of neutral winds in the mesosphere and lower thermosphere. Review of Scientific Instruments, 2004, 75, 2346-2350.	0.6	5
134	Comparison of winds measured by MU radar and Fabry–Perot interferometer and effect of OI5577 airglow height variations. Journal of Atmospheric and Solar-Terrestrial Physics, 2004, 66, 573-583.	0.6	14
135	Comparison of OH rotational temperatures measured by the spectral airglow temperature imager (SATI) and by a tilting-filter photometer. Journal of Atmospheric and Solar-Terrestrial Physics, 2004, 66, 891-897.	0.6	10
136	Mesosphere/lower thermosphere prevailing wind model. Advances in Space Research, 2004, 34, 1755-1762.	1.2	52
137	Atmospheric density and pressure inferred from the meteor diffusion coefficient and airglow O2b temperature in the MLT region. Earth, Planets and Space, 2004, 56, 249-258.	0.9	8
138	Simultaneous mesosphere/lower thermosphere and thermosphericFregion observations during geomagnetic storms. Journal of Geophysical Research, 2004, 109, .	3.3	15
139	Intraseasonal oscillations of the zonal wind near the mesopause observed with medium-frequency and meteor radars in the tropics. Journal of Geophysical Research, 2004, 109, n/a-n/a.	3.3	32
140	The 2-day wave during the boreal summer of 1994. Journal of Geophysical Research, 2004, 109, .	3.3	25
141	Interferometric meteor radar phase calibration using meteor echoes. Radio Science, 2004, 39, n/a-n/a.	0.8	24
142	Combined temperature lidar for measurements in the troposphere, stratosphere, and mesosphere. Applied Optics, 2004, 43, 2930.	2.1	78
143	Atmospheric wind effects on the gravity wave propagation observed at 22.7Ű S-Brazil. Advances in Space Research, 2003, 32, 819-824.	1.2	9
144	The lowest mesopause temperature in 1996 and 1997 at 23°S. Advances in Space Research, 2003, 32, 1781-1786.	1.2	3

#	Article	IF	CITATIONS
145	Lunar tidal winds in the upper atmosphere over Jakarta. Journal of Geophysical Research, 2003, 108, .	3.3	19
146	A localized structure in OH airglow images near the mesopause region. Journal of Geophysical Research, 2003, 108, .	3.3	8
147	Statistical study of short-period gravity waves in OH and OI nightglow images at two separated sites. Journal of Geophysical Research, 2003, 108, .	3.3	66
148	The 6.5-day wave in the mesosphere and lower thermosphere: Evidence for baroclinic/barotropic instability. Journal of Geophysical Research, 2003, 108, .	3.3	75
149	Equatorial Atmosphere Radar (EAR): System description and first results. Radio Science, 2003, 38, n/a-n/a.	0.8	147
150	Mesospheric gravity waves over a tropical convective region observed by OH airglow imaging in Indonesia. Geophysical Research Letters, 2003, 30, n/a-n/a.	1.5	75
151	Thermospheric wind during a storm-time large-scale traveling ionospheric disturbance. Journal of Geophysical Research, 2003, 108, .	3.3	46
152	Recent upgrades of the rotational vibrational-rotational Raman lidar of RASC, Kyoto University, Japan: first results. , 2003, , .		0
153	A two-channel Fabry-Perot interferometer with thermoelectric-cooled CCD detectors for neutral wind measurement in the upper atmosphere. Earth, Planets and Space, 2003, 55, 271-275.	0.9	41
154	TV Observation of the Leonid Meteor Shower in 2002: First Observation of a Faint Meteor Storm. Publication of the Astronomical Society of Japan, 2003, 55, 1157-1162.	1.0	5
155	Rotational vibrational-rotational Raman lidar: design and performance of the RASC Raman lidar at Shigaraki, Japan (34.8 degrees N, 136.1 degrees E). , 2002, , .		4
156	Calculation of the calibration constant of polarization lidar and its dependency on atmospheric temperature. Optics Express, 2002, 10, 805.	1.7	154
157	Combined Raman lidar for the measurement of atmospheric temperature, water vapor, particle extinction coefficient, and particle backscatter coefficient. Applied Optics, 2002, 41, 7657.	2.1	123
158	Convectively generated mesoscale gravity waves simulated throughout the middle atmosphere. Geophysical Research Letters, 2002, 29, 3-1.	1.5	97
159	First measurement of atmospheric density and pressure by meteor diffusion coefficient and airglow OH temperature in the mesopause region. Geophysical Research Letters, 2002, 29, 6-1-6-4.	1.5	19
160	Dual-site imaging observations of small-scale wave structures through OH and OI nightglow emissions. Geophysical Research Letters, 2002, 29, 85-1-85-4.	1.5	14
161	Horizontal structure of wind velocity field around the mesopause region derived from meteor radar observations. Journal of Atmospheric and Solar-Terrestrial Physics, 2002, 64, 947-958.	0.6	6
162	Global-scale tidal structure in the mesosphere and lower thermosphere during the PSMOS campaign of June–August 1999 and comparisons with the global-scale wave model. Journal of Atmospheric and Solar-Terrestrial Physics, 2002, 64, 1011-1035.	0.6	62

#	Article	IF	CITATIONS
163	Comparative study of interannual changes of the mean winds and gravity wave activity in the middle atmosphere over Japan, Central Europe and Canada. Journal of Atmospheric and Solar-Terrestrial Physics, 2002, 64, 1003-1010.	0.6	32
164	Long-Period wind oscillations in the mesosphere and lower thermosphere at Yamagawa (32°N,131°E), Pontianak (0°N,109°E) and Christmas Island (2°N,157°W). Journal of Atmospheric and Solar-Terrestrial Physics, 2002, 64, 1055-1067.	0.6	12
165	The wave2000 campaign: overview and preliminary results. Journal of Atmospheric and Solar-Terrestrial Physics, 2002, 64, 1095-1104.	0.6	10
166	Long-term variations of atmospheric wave activity in the mesosphere and lower thermosphere region over the equatorial Pacific. Journal of Atmospheric and Solar-Terrestrial Physics, 2002, 64, 1123-1129.	0.6	10
167	Breaking of small-scale gravity wave and transition to turbulence observed in OH airglow. Geophysical Research Letters, 2001, 28, 2153-2156.	1.5	81
168	Implications of meteor observations by the MU Radar. Geophysical Research Letters, 2001, 28, 1399-1402.	1.5	55
169	An improvement of wind velocity estimation from radar Doppler spectra in the upper mesosphere. Annales Geophysicae, 2001, 19, 837-843.	0.6	18
170	Seasonal variation of gravity waves with various temporal and horizontal scales in the MLT region observed with radar and airglow imaging. Advances in Space Research, 2001, 27, 1737-1742.	1.2	24
171	MF radar observations of mean winds over Yamagawa (31.2°N, 130.6°E) and Wakkanai (45.4°N, 141.7°E). Journal of Atmospheric and Solar-Terrestrial Physics, 2000, 62, 1177-1187.	0.6	11
172	Coordinated observations of the mesopause region with radar and optical techniques. Advances in Space Research, 2000, 26, 907-916.	1.2	4
173	Mesopause temperature observed by airglow OH spectra and meteor echoes at Shigaraki (34.9°N,) Tj ETQq1 1 ().784314 1.2	rgBT /Overlo
174	Gravity wave intensity and momentum fluxes in the mesosphere over Shigaraki, Japan (35°N, 136°E) during 1986-1997. Annales Geophysicae, 2000, 18, 834-843.	0.6	19
175	Average statistical characteristics of long gravity waves observed with the middle and upper atmosphere radar in the mesosphere. Journal of Geophysical Research, 2000, 105, 9365-9379.	3.3	10
176	Multi-point observation of short-period mesospheric gravity waves over Japan during the FRONT Campaign. Geophysical Research Letters, 2000, 27, 4057-4060.	1.5	17
177	Interannual variability of mesospheric mean winds observed with the MU radar. Journal of Atmospheric and Solar-Terrestrial Physics, 1999, 61, 1111-1122.	0.6	14
178	Seasonal variation of gravity waves observed with an OH CCD imager at Shigaraki (35°N,136°E), Japan. Advances in Space Research, 1999, 24, 561-564.	1.2	4
179	Wind observations in the MLT region over Southern Japan, by using foil chaff technique, Yamagawa MF radar and the NW radar. Advances in Space Research, 1999, 24, 575-578.	1.2	1
180	Observations of atmospheric waves in the tropical Pacific with radars and radiosondes. Advances in Space Research, 1999, 24, 1591-1600.	1.2	1

#	Article	IF	CITATIONS
181	Two-day wave structure and mean flow interactions observed by radar and High Resolution Doppler Imager. Journal of Geophysical Research, 1999, 104, 3953-3969.	3.3	47
182	Peculiarities of interannual changes in the mean wind and gravity wave characteristics in the mesosphere over Shigaraki, Japan. Geophysical Research Letters, 1999, 26, 2457-2460.	1.5	17
183	Coordinated radar observations of atmospheric diurnal tides in equatorial regions. Earth, Planets and Space, 1999, 51, 579-592.	0.9	33
184	Longitudinal variations in planetary wave activity in the equatorial mesosphere. Earth, Planets and Space, 1999, 51, 665-674.	0.9	50
185	Seasonal variations of 3.0â^1⁄43.8-day ultra-fast Kelvin waves observed with a meteor wind radar and radiosonde in Indonesia. Earth, Planets and Space, 1999, 51, 675-684.	0.9	52
186	Meteor observations with an MF radar. Earth, Planets and Space, 1999, 51, 691-699.	0.9	30
187	Cooperative wind observation in the upper mesosphere and lower thermosphere with foil chaff technique, the MU radar, and Yamagawa MF radar. Earth, Planets and Space, 1999, 51, 719-729.	0.9	11
188	Simultaneous measurements of dynamical structure in the mesopause region with lidars and MU radar. Earth, Planets and Space, 1999, 51, 731-739.	0.9	6
189	Observations of mesospheric sporadic sodium layers with the MU radar and sodium lidars. Earth, Planets and Space, 1999, 51, 785-797.	0.9	16
190	Response of the airglow OH emission, temperature and mesopause wind to the atmospheric wave propagation over Shigaraki, Japan. Earth, Planets and Space, 1999, 51, 863-875.	0.9	33
191	Development of Optical Mesosphere Thermosphere Imagers (OMTI). Earth, Planets and Space, 1999, 51, 887-896.	0.9	167
192	Seasonal variations of gravity wave structures in OH airglow with a CCD imager at Shigaraki. Earth, Planets and Space, 1999, 51, 897-906.	0.9	140
193	Simultaneous measurements of airglow oh emissionand meteor wind by a scanning photometer and the muradar. Journal of Atmospheric and Solar-Terrestrial Physics, 1998, 60, 1649-1668.	0.6	21
194	Meteor luminosity at 160 km altitude from TV observations for bright Leonid meteors. Geophysical Research Letters, 1998, 25, 285-288.	1.5	45
195	Propagation directions of gravity wave patterns observed in OH CCD images during the SEEK Campaign. Geophysical Research Letters, 1998, 25, 1793-1796.	1.5	17
196	HRDI Observations of Mean Meridional Winds at Solstice. Journals of the Atmospheric Sciences, 1998, 55, 1887-1896.	0.6	13
197	Statistical analysis of gravity waves observed with the middle and upper atmosphere radar in the middle atmosphere: 2. Waves propagated in different directions. Journal of Geophysical Research, 1997, 102, 13433-13440.	3.3	14
198	Development of an external interferometer for meteor wind observation attached to the MU radar. Radio Science, 1997, 32, 1203-1214.	0.8	10

Τακυji Νακαμυγά

#	Article	IF	CITATIONS
199	Seasonal and interannual variability of mesospheric echoes observed with the Middle and Upper Atmosphere Radar during 1986-1995. Geophysical Research Letters, 1997, 24, 1211-1214.	1.5	14
200	Coordinated global radar observations of tidal and planetary waves in the mesosphere and lower thermosphere during January 20-30, 1993. Journal of Geophysical Research, 1997, 102, 7307-7318.	3.3	16
201	Observations of diurnal oscillations with a meteor wind radar and radiosondes in Indonesia. Journal of Geophysical Research, 1997, 102, 26217-26224.	3.3	16
202	Short-period fluctuations of the diurnal tide observed with low-latitude MF and meteor radars during CADRE: Evidence for gravity wave/tidal interactions. Journal of Geophysical Research, 1997, 102, 26225-26238.	3.3	51
203	Radar observations of a 3-day Kelvin wave in the equatorial mesosphere. Journal of Geophysical Research, 1997, 102, 26141-26157.	3.3	79
204	An intercomparison between the GSWM, UARS, and ground based radar observations: a case-study in January 1993. Annales Geophysicae, 1997, 15, 1123-1141.	0.6	41
205	Validation of HRDI MLT winds with meteor radars. Annales Geophysicae, 1997, 15, 1142-1157.	0.6	13
206	Simultaneous observations of mesospheric gravity waves with the MU radar and a sodium lidar. Journal of Geophysical Research, 1996, 101, 4057-4063.	3.3	26
207	Wind velocity and temperature fluctuations due to a 2-day wave observed with radio meteor echoes. Journal of Geophysical Research, 1996, 101, 9425-9432.	3.3	24
208	Mesospheric gravity waves at Saskatoon (52°N), Kyoto (35°N), and Adelaide (35°S). Journal of Geophysical Research, 1996, 101, 7005-7012.	3.3	45
209	Phase calibration of VHF spatial interferometry radars using stellar sources. Radio Science, 1996, 31, 147-156.	0.8	15
210	Comparison of wind measurements between Yamagawa MF Radar and the MU Radar. Geophysical Research Letters, 1996, 23, 3341-3344.	1.5	31
211	Statistical analysis of gravity waves observed with the middle and upper atmosphere radar in the middle atmosphere: 1. Method and general characteristics. Journal of Geophysical Research, 1996, 101, 29511-29521.	3.3	50
212	Mean winds at 60–90 km observed with the MU radar (35°N). Journal of Atmospheric and Solar-Terrestrial Physics, 1996, 58, 655-660.	0.9	21
213	A Preliminary Report on Observations of Equatorial Atmosphere Dynamics in Indonesia with Radars and Radiosondes. Journal of the Meteorological Society of Japan, 1995, 73, 393-406.	0.7	39
214	Simultaneous observations of meteors with the radar and TV systems. Earth, Moon and Planets, 1995, 68, 277-282.	0.3	9
215	Diurnal variations of the planetary boundary layer observed with anL-band clear-air doppler radar. Boundary-Layer Meteorology, 1995, 74, 419-424.	1.2	31
216	The effects of particle size distributions on cross-spectral phase measurements in spatial interferometry. Radio Science, 1995, 30, 1065-1083.	0.8	3

#	Article	IF	CITATIONS
217	Weighted imaging Doppler interferometry. Radio Science, 1995, 30, 1787-1801.	0.8	4
218	High-resolution wind profiling using combined spatial and frequency domain interferometry. Radio Science, 1995, 30, 1665-1679.	0.8	14
219	Features of a mesospheric inertio-gravity wave observed with the MU radar. Journal of Atmospheric and Solar-Terrestrial Physics, 1994, 56, 1163-1171.	0.9	5
220	Variations of the gravity wave characteristics with height, season and latitude revealed by comparative observations. Journal of Atmospheric and Solar-Terrestrial Physics, 1994, 56, 555-568.	0.9	83
221	Temperature fluctuations near the mesopause inferred from meteor observations with the middle and upper atmosphere radar. Radio Science, 1994, 29, 599-610.	0.8	78
222	Middle and upper atmosphere radar observations of ionospheric density gradients produced by gravity wave packets. Journal of Geophysical Research, 1994, 99, 6321.	3.3	34
223	Reply [to "Comments on â€~Middle and upper atmosphere radar observations of ionospheric density gradients produced by gravity wave packets' by W. L. Oliver et al.â€]. Journal of Geophysical Research, 1994, 99, 21415.	3.3	0
224	Seasonal variability of vertical eddy diffusivity in the middle atmosphere: 1. Three-year observations by the middle and upper atmosphere radar. Journal of Geophysical Research, 1994, 99, 18973.	3.3	202
225	Middle and upper atmosphere radar observations of ionospheric horizontal gradients produced by gravity waves. Journal of Geophysical Research, 1993, 98, 9443-9451.	3.3	21
226	Characteristics of gravity waves in the mesosphere observed with the middle and upper atmosphere radar: 1. Momentum flux. Journal of Geophysical Research, 1993, 98, 8899-8910.	3.3	77
227	Characteristics of gravity waves in the mesosphere observed with the middle and upper atmosphere radar: 2. Propagation direction. Journal of Geophysical Research, 1993, 98, 8911-8923.	3.3	48
228	Comparison of the mesospheric gravity waves observed with the MU Radar (35°N) and the Adelaide MF Radar (35°S). Geophysical Research Letters, 1993, 20, 803-806.	1.5	16
229	Comparative observations of shortâ€period gravity waves (10–100 min) in the mesosphere in 1989 by Saskatoon MF radar (52°N), Canada and the MU radar (35°N), Japan. Radio Science, 1993, 28, 729-746.	0.8	32
230	Dominant vertical scales of gravity waves in the middle atmosphere observed with the MU radar and rocketsondes. Journal of Atmospheric and Solar-Terrestrial Physics, 1992, 54, 339-346.	0.9	22
231	Rocketsonde Observations of the Middle Atmosphere Dynamics at Uchinoura(31.DEG.N,131.DEG.E) during the DYANA Campaign. Part II: Characteristics of Gravity Waves Journal of Geomagnetism and Geoelectricity, 1992, 44, 1009-1023.	0.8	18
232	Rocktsonde Observations of the Middle Atmosphere Dynamics at Uchinoura(31.DEG.N,131.DEG.E) during the DYANA Campaign. Part I: Outline of Experiments and Background Conditions Journal of Geomagnetism and Geoelectricity, 1992, 44, 995-1007.	0.8	8
233	Meteor wind observations with the MU radar. Radio Science, 1991, 26, 857-869.	0.8	73
234	Multiple beam observations of mid-latitude ionospheric disturbances by the MU radar. Journal of Atmospheric and Solar-Terrestrial Physics, 1991, 53, 773-779.	0.9	7

#	Article	IF	CITATIONS
235	Frequency spectra of mesospheric wind fluctuations observed with the MU radar. Geophysical Research Letters, 1990, 17, 1897-1900.	1.5	15
236	A MU radarâ€based study of midâ€latitude <i>F</i> region response to a geomagnetic disturbance. Journal of Geophysical Research, 1990, 95, 21077-21094.	3.3	36
237	Mean winds observed by the Kyoto meteor radar in 1983–1985. Journal of Atmospheric and Solar-Terrestrial Physics, 1987, 49, 461-466.	0.9	37